

Microcosm analysis of the impact of nutrients and allochthonous carbon on microbial production
of autotrophic and heterotrophic biomass

Hilary Smith
Ripon College, 600 Campus Dr., Ripon, WI 54971

Advisor
Dr. Joe Vallino
Ecosystems Center, Marine Biological Laboratory, 7 MBL St., Woods Hole, MA 02543

19 December 2005

Abstract.

Microorganisms play a primary role in the maintenance of life, performing essentially all biochemical reactions that occur on earth, producing large quantities of oxygen through photosynthesis, engaging in symbioses, and regenerating nutrients through the decomposition of organic matter. Considering microbes' critical importance to the planet's biogeochemistry and their support of higher life forms, it is essential to further understand microbial communities. Moreover, studies of microbial communities can provide knowledge of general principles governing community dynamics that may be used in examining the way in which communities and ecosystems develop. Thus, I have examined microbial metabolism in microcosms, analyzing carbon, nitrogen, and oxygen concentrations to analyze the formation of autotrophic and heterotrophic biomass. Based on the goal function of Maximum Entropy Production (MEP), I have hypothesized that living systems will preferentially allocate biomass to heterotrophic structures to maximize energy degradation and entropy production. According to MEP, living systems act to restore the planet to its original state of high entropy and low energy by dissipating solar and chemical energy gradients. I found that systems provided with light energy in a growth chamber, and with daily pulses of chemical energy in the form of glucose, allocated most of their resources to heterotrophic degradation of glucose. This trend held for varying nutrient treatments in two experiments, with daily carbon additions that greatly exceeded nutrient additions in the first experiment, and a very low ratio of carbon to added nutrients in one treatment of the second experiment. My general discovery of heterotrophic dominance supports my expectations based on MEP, despite the unexpected result that systems with nutrients in excess of the requirements of heterotrophs did not always use their remaining resources for autotrophic degradation of light energy. Further research is needed to determine whether MEP truly applies to these systems, and research should be conducted for longer than the 12 d of each of my experiments to ensure that the communities have stabilized before they are examined.

KEYWORDS:

Microcosms; microbes; maximum entropy production; autotrophs; heterotrophs; allocation of biomass; respiration; dissolved oxygen

INTRODUCTION

Microorganisms range from endosymbionts that enable ruminants to digest plant material (particularly cellulose) and zooxanthellae that provide corals with energy, to a plethora of aquatic and terrestrial microbes that decompose organic matter and release nutrients for use by other organisms. Microbes not only prepared the earth for the evolution of higher life forms, but also support the survival of these organisms (Madigan et. al. 2000). For instance, microbial production of free oxygen was necessary for the later development of eukaryotes (Schlesinger 1997). Moreover, microbial processes largely govern the earth's biogeochemical cycles (Vallino 2003). Thus, understanding the activities of microbes is essential to understanding the cycling of nutrients vital to life.

The sheer abundance of microbes further reveals their importance. Whitman and colleagues (1998) suggest that over half of the world's living matter is microbial. Microbes' abundance and small size make them useful in examining community dynamics. It is estimated that 1 mL of water contains 1 million microbes, and the many microbes that can be cultivated in a small container represent an enormous diversity of metabolic pathways. Many bacterial populations double in 1-3 h (Madigan et. al. 2000). This fast reproduction rate facilitates the rapid mutation of microorganisms and their ability to quickly adapt to ambient environmental

conditions, allowing for observations of evolutionary change and community development over relatively short time scales. Microbial analyses are used to expand our knowledge of general biological principles, including inheritance, biochemistry, and the cycling of gases, minerals, and nutrients (Talaro 2005).

In this investigation, I have used microbes to examine the concept of maximum entropy production (MEP) and its application to living systems. This hypothesis stems from Schrödinger's explanation of nonequilibrium thermodynamics (1945). Schrödinger clarified organized living systems' apparent violation of the second law of thermodynamics by noting that open systems utilize an outside energy source to create order, and in so doing increase the disorder of the outside system to an equal or greater degree. Swenson applied this concept in asserting that the universe operates to maximize entropy production (Salthe 2003). Schneider and Kay (1994) further note that when moved from a state of equilibrium through the establishment of gradients, systems respond so as to dissipate these gradients. In an attempt to provide a fundamental principle to guide ecological studies, they propose that living systems can be viewed as structures designed to degrade inputs of chemical potential and solar energy. By dissipating energy, systems gain from the work performed during the degradation process, and this ability to do work can be considered a selective advantage for biological systems (Fath et. al. 2001). Thus, in accordance with the concept of MEP, ecosystems develop to maximize energy degradation and entropy production, thereby restoring thermodynamic equilibrium.

The MEP hypothesis is significant in that it provides a basis for predicting the way in which ecosystems and communities develop, applying a holistic view to ecosystem research. This concept extends beyond Darwin's theory for the selection of individual species to a goal function for the selection of ecosystems. While MEP could be analyzed with regard to any organism, I analyzed microbial communities due to their aforementioned utility in studies of general biological principles. The existence of microbial consortia reveals the interconnectedness of microbial communities and is suggestive of the potential for an overall goal that governs community structure and function. Hashsham and colleagues (2000) define microbial communities functionally as a metabolic network comprised by the activities of interdependent populations. As an example, hydrogen gas produced by microbial fermentative degradation of organic matter in anoxic sediments is consumed by methanogens, which produce methane that diffuses upward and is oxidized by methanotrophs (Madigan et. al. 2000). Additionally, the swarming of *Proteus* and *Serratia* spp. provides evidence of coordinated multicellular activity (Shapiro 1998). The concept of MEP can be applied as a theoretical model for understanding the formation of these communities.

Due to the relative simplicity of microcosms in comparison with complex, heterogeneous ecosystems subject to many uncontrollable variables, I used microcosms to analyze the organization of microbial systems in accordance with the hypothesis of MEP. While a microcosm is not representative of any particular ecosystem, it is itself a living system, and thus should be governed by MEP or any other general principles dictating the development of living systems. The concept of MEP is useful as a theoretical framework for addressing such questions as resource allocation, and predicts that systems will allocate resources to maximize energy degradation. I hypothesize that heterotrophs are more efficient at degrading energy than autotrophs, and are selected for in ecosystems with sufficient resources to sustain their activity. This expectation is based on the fact that autotrophs must use solar energy and biomass to synthesize organic matter before degrading it, while heterotrophs directly consume and degrade preformed organic matter. Because nutrients are required for the formation of biomass, nutrients

are an important factor in the development of autotrophic and heterotrophic structures. When limited by nutrients, I predict that systems will allocate all of their resources to heterotrophic biomass. When nutrients are provided in excess of that needed for heterotrophic oxidation of organic matter, I predict the system will allocate its remaining resources to autotrophic biomass for degradation of light energy. I have applied the concept of MEP and an analysis of particulate organic matter, dissolved organic matter, and oxygen concentrations in microcosms to address the relation between concentrations of nutrients (nitrogen, phosphorous, and silica) and the allocation of microbial biomass to autotrophic and heterotrophic structures.

METHODS

Initially, I monitored the piston velocity (kL) of the diffusion of oxygen into a 5 gal. plastic bucket filled with 18.16 L of seawater. I collected the water for monitoring piston velocity approximately 0.3-0.6 m off a dock at Eel Pond in Woods Hole, MA. I noted the oxygen concentration after allowing the water to sit at room temperature for 2 d to reach equilibrium with the oxygen content of the overlying air (O_2^*). I then sparged the seawater with nitrogen gas until the oxygen concentration reached approximately 0 mg/L. By graphing the diffusion of oxygen back into the bucket over time, and multiplying the exponent of the trendline by the height of the water (0.316 m), I determined the piston velocity (Fig. 1). I then used this value to calculate the rate of oxygen diffusion into the water using the following equation:

$$Rate = kL/h(O_2^* - O_2)$$

where h is the height of the water in the bucket (0.0279 m). The current oxygen concentration (O_2) was 0 mg/L due to the bubbling with nitrogen. I also conducted this experiment with a bucket of artificial seawater allowed to equilibrate with air overnight (Fig. 2), and used the average of the two values for piston velocity to calculate the rate of diffusion of oxygen.

After measuring piston velocity, I performed two separate microcosm experiments in containers identical to the white bucket in which I had measured the piston velocity. All inoculums were collected from the same side of the dock at Eel Pond where water was collected to measure piston velocity. I homogenized the water collected for the second experiment prior to establishing the individual treatments because the water in different buckets was different shades of green, implying differing initial concentrations of autotrophs and chlorophyll. The bucket for monitoring piston velocity and the buckets in which I established the microcosms were kept on stir plates, and stirred with an approximately 5 cm stir bar at speeds that created a vortex of about 1-2 cm.

In both microcosm experiments, I incubated all microcosms at 20°C for approximately 12 d in a Conviron growth chamber (Controlled Environments Limited, model PGR-15). As an energy source, all microcosms received 12 h of light daily at approximately 1248 PAR, as measured with a Hydrolab® Data Sonde® 4 Water Quality Multiprobe (Hydrolab Corporation). In the first experiment all microcosms received 400 $\mu\text{M C/d}$ as glucose on the first day, and 2400 $\mu\text{M C/d}$ thereafter. I added 400 $\mu\text{M C/d}$ in the form of glucose to all microcosms throughout the second experiment. These glucose concentrations were based on the original volume of 18.16 L prior to removal of water for sample collection; incoming energy per unit water in the form of glucose and light increased during the experiment. Although glucose was added to the initial set of microcosms in the evening on the first two days, all further additions for the first experiment, and all additions in the second experiment, were made in the morning near the time when the lights came on in the growth chamber.

In each experiment, I added nitrogen, silica, and phosphorous to the microcosms within 24 h of placing them in the growth chamber. In contrast to the glucose additions, nutrients were only added once to each microcosm. With the eight microcosms I established in the first experiment, I conducted four nutrient treatments in replicate (Table 1), and in the second experiment I established three nutrient treatments in replicate (Table 2). Additions of nutrients in both experiments were based on the Redfield molar ratio of 16 N:1 P, and a ratio of 3 Si:2 N. Although nitrogen and phosphorous are typically thought of as the primary limiting nutrients in ecosystems, with nitrogen viewed as the most limiting nutrient in oceans, silica can limit diatom growth. Concentrations of silica are often less than 2 μM at the ocean's surface (Schlesinger 1997). Gilpin and colleagues (2003) note that the Redfield ratio for N:Si ratio is 1:1. Citing Brzezinski; however, they reveal that the ratio for the diatom *Skeletonema costatum* reached a ratio of 1.5 when it received continuous light. Hence, I added silica as well as nitrogen and phosphorous, and used a 1.5 ratio of N:Si in my nutrient additions.

Throughout each experiment, I measured the concentration of dissolved oxygen (DO) in each microcosm twice daily, immediately prior to when the lights turned on and off. Oxygen measurements were made with a WTW Pocket Oxygen Meter (model 340i), and calibrations were performed in air saturated with water vapor using the OxiCal®-SL air calibration vessel. Total system respiration (R) was calculated for the first experiment as follows:

$$R = (O_2(tm2) - O_2(te1)) / (tm2 - te1) - kL/h * [O_2^* - (O_2(te1) + O_2(tm2))/2]$$

where *tm2* refers to the time at which oxygen is measured on the morning of the second day, and *te1* refers to the time at which oxygen is measured on the evening of the first day. Respiration during the day and night was assumed to be equal in the first experiment. However, in the second experiment I covered the second replicate of microcosms with black plastic trash bags to exclude light at 7-9 d after the initial nutrient addition. Based on the lack of any oxygen production in microcosms receiving light compared with those in the dark, and the absence of a significant change in the average daily DO concentrations, respiration in treatments A and C was presumed to consume all oxygen diffusing into the buckets, and was calculated using the following equation:

$$R = kL/h * [O_2^* - O_2(avg)].$$

Values for $O_2(avg)$ were based on the average DO values throughout these three days, at approximately 240 μM O_2 and 100 μM O_2 in the A and C treatments, respectively. I determined the average respiration for treatment B with the same equation used in the first experiment due to the constant DO values seen in the dark treatment, which implied equal respiration during the day and night. For both experiments, net productivity (NP) between the time at which the lights turned on (*ton*) and turned off (*toff*) was calculated as follows:

$$NP = (O_2(te1) - O_2(tm1)) / (te1 - tm1) * (toff - ton) / 1.0 - kL/h * [O_2^* - (O_2(tm1) + O_2(te1))/2]$$

where *tm1* refers to the morning of the first day. Finally, I calculated gross productivity (GP) in each experiment using the equation:

$$GP = NP - R.$$

In addition to monitoring DO, I also collected and preserved samples for analysis of chl *a*, particulate organic carbon and nitrogen (POC, PON) dissolved organic carbon (DOC), nitrate, and ammonium. I collected chl *a*, POC, and PON samples by two methods. Initially, I used vacuum filtration to collect chl *a* samples on 47 mm Whatman filters that had not been ashed. Samples were then extracted and analyzed in accordance with the methods of Lorenzen (1967) on a UV/VIS Spectrometer (Perkin Elmer, model Lambda Bio 120). To analyze particulate organic matter (POM) I collected samples on ashed 25 mm Whatman GF/F filters with vacuum

filtration, and combusted the filters on a Series II CHNS/O Analyzer (Perkin Elmer, model 2400). However, for the final chl *a* and POM measurements for treatments C and D in the first experiment, and the final two measurements for microcosms B and C in the second experiment, centrifugation was used to collect samples. For these samples, a significant volume of water could not be filtered for analysis of chl *a* and POM due to the density of the microbial populations, which caused the filter to clog. I centrifuged 50-100 mL of sample for 1 h/50 mL of sample on an Allegra™ 25R Centrifuge (Becker Coulter) at 5000 g with a TS-5.1-500 rotor. The pellet and approximately 3.5 mL of supernatant were left in the centrifuge tube and extracted with 100% acetone for chl *a* analysis using the protocol of Lorenzen (1967). I collected another pellet, re-suspended it in approximately 1-2 mL of deionized water, and poured it onto an ashed 25 mm Whatman GF/F filter to analyze POC and PON.

For the final sample from all microcosms in the first experiment, and the final two samples from the second experiment, the supernatant from centrifugation was used for measurements of DOC, nitrate, and ammonium. All other samples of DOC, nitrate, and ammonium were collected by passing water samples through a 25 mm ashed Whatman GF/F filter using a syringe and Swinex filter holder. For DOC analysis, samples were preserved and analyzed according to the protocol of Peltzer and Brewer (1993) using high-temperature catalytic oxidation on a DOC analyzer constructed according to their description. Nitrate samples were frozen for preservation until analysis with the Lachat Quik-Chem 8000 (Lachat Instruments). After preservation of 10 mL of sample with 10 μ L of 5 N HCl, ammonium was analyzed using the phenolhypochlorite method (Solórzano 1969). Reagents used in the ammonium analysis were slightly modified. I used the equivalent of 20 g rather than 10 g of crystalline phenol dissolved in 100 mL of 95% v/v ethyl alcohol, and 5 g of nitroprusside dissolved in 10 mL of deionized water rather than 1 g in 200 mL of water. I analyzed ammonium concentrations with a UV-1601 UV-Visible Spectrophotometer (Shimadzu).

RESULTS

I determined that the piston velocity for a bucket of water from Eel Pond (Fig. 1) and a bucket of artificial seawater (Fig. 2) were 0.84 m/d and 0.65 m/d, respectively, for an average of 0.75 m/d. Based on this average, I determined that the initial rate of oxygen diffusion into my microcosms was 652 μ M O₂ m/d, based on the equilibrium oxygen concentration of seawater that I measured as 240 μ M O₂. At this rate and a 1:1 ratio of glucose consumed to oxygen depleted, complete oxidation of the 2400 μ M C added daily in the first experiment would exceed the rate of diffusion of oxygen, whereas complete oxidation of the 400 μ M C/d added in the second experiment would not exceed the rate of diffusion. In the first experiment only the D treatment experienced anoxia (Fig. 3), and in the second experiment DO concentrations remained well above 0 μ M for all treatments (Fig. 4).

All values reported for the first experiment reflect the average values of the two microcosms for treatments A and B, with the second microcosm of treatments C and D excluded from the results due to errors in the initial nutrient additions (Table 1). Values of R, NP, and GP in the first experiment represent the average value 7-12 d after nutrient additions. For the second experiment, all values for each treatment (Table 2) represent the average for the two replicate microcosms, except for the calculations of R, NP, and GP. These calculations are based on the average oxygen concentration 7-9 d after nutrient additions for the first replicate of microcosms, which were not excluded from the light. For all measurements, time zero represents the time of the initial nutrient addition.

In the first experiment, essentially all inorganic nitrogen present after nutrient additions appeared to be metabolized, while glucose, or DOC, accumulated. There was a sharp decline in concentrations of ammonium and nitrate, with nearly complete depletion of each by the fourth day in all microcosms (Fig. 5). The sum of nitrate and ammonium concentrations remained negligible for the remainder of the experiment. Measured concentrations of DOC in the first experiment exceeded the total DOC added in treatments A and B (Fig. 6). For all microcosms, DOC values rose over time, revealing the presence of a large pool of glucose.

Levels of DO in the first experiment showed large fluctuations before stabilizing on the after 6 d. Following stabilization, DO remained fairly constant for the remainder of the incubation, and there was no diurnal oxygen cycle. In comparing the treatments after stabilization, I observed that concentrations of DO were less and respiratory activity higher (Fig. 7) for treatments with higher nutrient additions. Despite the NP of $28 \mu\text{M O}_2/\text{d}$ in the A treatment, values of NP typically were negative and equal to R. With NP approximately the same as R, GP was about $0 \mu\text{M O}_2/\text{d}$. Also, I estimated autotrophic carbon biomass from my measurements of chl *a* and an assumed ratio of $50 \mu\text{g C}:1 \mu\text{g chl } a$. In the first experiment, autotrophic carbon declined in all but the C treatment between my initial measurement and my final measurement 12.5 d later, with a peak in autotrophic biomass after 9 d in the C and D treatments (Fig. 8). However, this autotrophic carbon comprised a minor component of the total carbon biomass present as POC (Fig. 9).

Similar to the results of the first experiment, nitrate and ammonium concentrations reached $0 \mu\text{M}$ after 5-6 d for treatments A (Fig. 10) and B (Fig. 11). In the C treatment; however, the nitrate concentration measured on the sixth day had declined by a mere $63.5 \mu\text{M}$ from the original measured concentration (Fig. 12). A small amount of ammonium was produced over time, but the $5.8 \mu\text{M}$ increase in ammonium clearly was insufficient to account for the majority of the nitrate depletion. Meanwhile, measured DOC concentrations for all treatments were less than that of the DOC added as glucose. Concentrations of DOC were highest for the A treatment (Fig. 10). The DOC concentrations for the B and C treatments were approximately equal, with both treatments consuming essentially all DOC added as glucose between the fifth and sixth days.

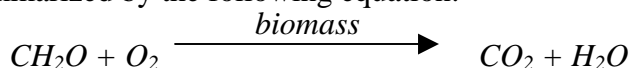
As in the first experiment, all microcosms in the second experiment appeared to reach a steady metabolic state by 6 d after nutrient additions, as seen in their constant values for DO over time (despite diurnal fluctuations). No diurnal variations in oxygen were seen in the A treatment of the second experiment, but the C treatment of this experiment showed an inverted diurnal oxygen cycle after stabilization, with DO values rising at night and declining in the day. The B treatment exhibited this inverted cycle initially, but after stabilizing it transitioned to the typical cycle of increasing oxygen during the day and declining values at night. After covering one microcosm in each treatment, I found that the DO in the A and C treatments showed no significant difference for microcosms in the light and dark, whereas covering one of the two B treatment microcosms caused a shift from its diurnal oxygen cycle to a constant DO concentration. Although there were fluctuations in DO between day and night for the C treatment, I determined that GP of oxygen was $0 \mu\text{M}/\text{d}$ in the A and C treatments due to the fairly constant DO values between one 24 h day and the next (Fig. 14). Because exclusion from light did not impact the DO concentrations of these treatments, I assumed that no oxygen was produced by autotrophy. Furthermore, all oxygen entering the buckets through diffusion must have been consumed since DO concentrations neither increased nor decreased significantly over time. Given the negative values for R (equal to the diffusion of oxygen for treatments A and C)

and the requirement that $NP = R$ to attain a GP of $0 \mu\text{M}/\text{d}$, NP of oxygen was negative for these treatments. While R and NP were negative for treatment B as well, this treatment had a positive GP of $66 \mu\text{M O}_2/\text{d}$ based on the methods for calculating R, NP, and GP used in the first experiment. As in the first experiment, respiratory consumption of oxygen increased with increasing nutrient additions in the microcosms. There was a small rise in autotrophic carbon biomass over time in the A and C treatments, and an increase of over 400% in the B treatment (Fig. 15). Autotrophic carbon comprised a minor component of total system biomass in treatments A and C. However, there was a large variation in the POC measurement for the two microcosms from treatment C, as seen in the large standard deviation (Fig. 16). Autotrophic carbon slightly exceeded measured POC in the B treatment.

Overall, increasing nutrient concentrations initially yielded a larger quantity of biomass in the form of nitrogen, estimated as PON. This positive relationship was seen in both the first (Fig. 17) and second (Fig. 18) experiments. However, there was a small decrease in PON formation relative to initial DIN concentration (estimated as the sum of nitrate and ammonium) for treatment B, and a large standard deviation for the PON measurement for treatment C of the second experiment. For all treatments, PON formed by 12 d and 5 d in the first and second experiments, respectively, was significantly less than the total DIN. Data collected for nitrogen in living biomass exhibited a strong positive relationship with respiration for the first experiment (Fig. 19). Respiration increased for higher concentrations of PON in the second experiment as well (Fig. 20), although the relation between PON and respiration appeared more variable due to the seemingly low value of PON for treatment B and the large standard deviation of treatment C.

DISCUSSION

Although formation of biomass typically might be viewed as the end result of system organization, I have considered the biomass of microcosms as a catalyst in the overall reaction of energy degradation, summarized by the following equation:



I anticipated that heterotrophic biomass would be a more effective catalyst for the above reaction due to heterotrophs' ability to directly degrade organic matter, as contrasted with autotrophic metabolism. Autotrophs must use biomass and resources to convert solar energy into organic matter before this reaction can proceed. Thus, I expected preferential development of heterotrophic structures based on the hypothesis of MEP, which states that systems organize to maximize energy degradation and entropy production.

In the first experiment, glucose additions in the four treatments (Table 1) clearly occurred at a rate greater than or equal to the nutrient requirement of the system for generating biomass to catalyze energy degradation. This is implied by the rapid decline of dissolved inorganic nitrogen (DIN), estimated as the sum of ammonium and nitrate (Fig. 5). The lack of a significant quantity of DIN in the water implies that all added nitrogen had been used by microbes. Yet, for both experiments, the relatively low amount of PON formed in comparison with the initial DIN concentration suggests that much of this nitrate may have been converted to dissolved organic nitrogen, or some other unmeasured form of nitrogen (Figs. 17, 18). Because only the D treatment of the first experiment experienced anoxia, this treatment probably is the only one that could have allowed for significant depletion of nitrate by denitrification. All treatments' glucose levels clearly increased throughout the first experiment, with measured DOC actually exceeding the amount of glucose added in the A and B treatments (Fig. 6). In fact, measured DOC after 12 d exceeded that added to the A treatment by $2817 \mu\text{M}$, and surpassed DOC additions to the B

treatment by 1810 μM . The excess of measured DOC over that added suggests that there was an error in the measurement of the absolute concentration of DOC. Nonetheless, I did find a decrease in the relative DOC values for treatments that had received more nutrients, presumably due to the ability of the extra nutrients to support more biomass for glucose oxidation. However, the general increase in DOC and depletion of DIN implied that insufficient nutrients were present to meet heterotrophic needs for complete glucose oxidation.

In this first experiment, my expectation of preferential development of heterotrophic biomass to degrade energy gradients, and of complete heterotrophy in systems limited by nutrients, was clearly supported in all four nutrient treatments. After stabilization, DO concentrations remained constant (Fig. 3) and oxygen consumption by respiration was approximately equal to, or greater than, the calculated values of NP (Fig. 7). Respiration increased as more nutrients were added, with more nutrients enabling the system to form more biomass to catalyze the degradation of energy. Values for GP remained near 0 $\mu\text{M O}_2/\text{d}$ after stabilization in all treatments, revealing that the systems were primarily heterotrophic. Applying the estimated ratio of 50 $\mu\text{g C}$: 1 $\mu\text{g chl } a$ to my measurements of chl *a* further revealed a small increase in autotrophic carbon biomass during the experiment (Fig. 8). Autotrophic carbon biomass was a small component of the total carbon biomass, with the latter estimated by measurements of POC (Fig. 9). The ratio of carbon to chl *a* of autotrophs is variable, with the range for phytoplankton reported at 22 to 154 (Valiela 1995), and POC values reflect the sum of both dead and living organic matter. Despite these limitations of the comparison, the great excess of POC in comparison to chl *a* suggests that few resources were devoted to autotrophic structures for light degradation, despite uncertainty of the exact amount of autotrophic biomass and the portion of POC representing live biomass. Also, while I only determined the presence of autotrophic carbon based on measurements of chl *a*, the GP of 0 $\mu\text{M O}_2/\text{d}$ suggests that aerobic primary producers utilizing pigments other than chl *a* did not comprise a large component of the microbial community.

Unlike my first experiment, the results of my second experiment suggest nutrient additions (Table 2) were in excess of heterotrophic requirements for oxidizing the 400 $\mu\text{M C}$ added daily and any autochthonous DOC present in the microcosms. While metabolic activity appeared to consume nearly all DIN in the A and B treatments (Figs. 10, 11), nutrient additions clearly exceeded heterotrophic ability to consume nitrogen in my C treatment, with a decrease in the nitrate concentration of only 63.5 μM in 6 d (Fig. 12). This decline in nitrate concentration for the C treatment was near that of the B treatment, in which essentially none of the 85 μM nitrate measured initially remained after 6 d. Furthermore, daily glucose additions did not appear to exceed the capacity of the system for oxidation in the B and C treatments. Whereas DOC accumulated in treatment A, the B and C treatments showed no significant change in DOC values between the fifth and sixth days, implying essentially complete oxidation of the glucose added daily (Fig. 13). Moreover, the decreased DO values of treatment C during the day, which likely reflect increased respiration following the addition of glucose in the morning, revealed that the system contained less DOC than it was capable of oxidizing. Hence, while the microbial communities in my first experiment and treatment A of my second experiment appeared limited by nutrients, treatment C had an excess of added nutrients relative to allochthonous carbon, and treatment B had at least as many nutrients as were required to degrade the added glucose.

As in the first experiment, the overall results of my second experiment suggested that the system preferentially allocated resources to formation of heterotrophic biomass. The GP of 0 $\mu\text{M}/\text{d}$ in the A and C treatments (Fig. 14), which indicated the absence of a large autotrophic

community, and the minimal contribution of autotrophic carbon to the total carbon biomass (Fig. 16), revealed the dominance of heterotrophic structures for degradation of preformed organic matter. However, the lack of a large presence of autotrophs in the C treatment was unexpected due to the apparent excess of nutrients. It is possible that trace elements or some other resource required to form biomass became limiting to growth despite the excess nitrogen available to form biomass and the likely (but unmeasured) excess of phosphorous and silica. For instance, a trace nutrient such as iron or magnesium could have limited biomass development beyond the formation of heterotrophic structures. Further experiments designed to ensure that all resources needed for biomass development clearly exceed the availability of DOC in the system should be conducted to explore the possibility for formation of autotrophic biomass as a secondary catalyst for energy degradation. However, the results of both of my experiments indicated that heterotrophic biomass is selected for as the primary catalyst when systems are provided with sufficient organic matter to support heterotrophy. In all, the results of my first experiment and treatment A of the second experiment are consistent with my expected results based on the hypothesis of MEP, though the results when nutrients are added in excess of heterotrophic needs requires further clarification.

Despite the overall concurrence of the results with my expectation for preferential development of heterotrophic biomass, I did witness a surprisingly high autotrophic component in the treatment B microbial community of the second experiment considering the absence of autotrophy in treatment C. Autotrophic carbon clearly increased over time for treatment B (Fig. 15). Measured autotrophic carbon exceeded the total carbon biomass, implying the importance of autotrophy to the metabolism of this system (and a potential error in either the measurement of POC or the estimated ratio of carbon to chl *a* given that autotrophic carbon should not exceed total POC). If sufficient nutrients were available in the B treatment to support heterotrophic and autotrophic biomass, it seems unlikely that C treatment, with a tenfold increase in nitrogen, phosphorous, and silica additions, would have experienced sufficient resource limitation to prevent formation of autotrophic structures. Yet, measurements of the initial concentrations of trace nutrients and other resources would need to be conducted to ensure that they were equally available in both treatments. Because there was sufficient heterotrophic biomass to oxidize glucose and prevent an accumulation of DOC, my prediction for the development of heterotrophic structures is applicable to my observations. Still, my expectation for the allocation of excess resources to autotrophy based on MEP may not apply to these microcosms. Additional research is necessary to determine whether my results can be interpreted as refuting my prediction, or whether the experiment itself should be modified to show the true response of systems to high nutrient concentrations.

Notably, the hypothesis of MEP, and my prediction of preferential formation of heterotrophic biomass, applies to systems in a steady state. Additional observations of the B treatments over time, and of all other treatments, should be conducted to ensure that they have stabilized and the observed results can be applied to my hypothesis. While the C treatment appeared to respire all of the 400 μM C added daily, with R at 452 μM O_2/d and no accumulation of DOC between the fifth and sixth days despite the daily glucose addition, the B treatment appeared to be in a state of continuing biomass formation. Respiration for the B treatment merely averaged 173 μM O_2/d after stabilization, while all DOC added between the fifth and sixth days appeared to be consumed. The low value of R relative to daily DOC consumption at this time suggested that much of the glucose was being used for biomass formation, and that the system may not have stabilized with respect to the total biomass it could form for degradation of energy.

The relatively low POC and PON values for this system further indicated that biomass formation was incomplete, with far less POC and PON in treatment B than in treatment A, despite the presence of more nutrients to support biomass formation in treatment B. In the short time frame of this experiment, it is possible that my results were influenced by a species effect, and may reflect a large phytoplankton community initially present in the B treatment that allowed for the significant amount of autotrophy. If later observations revealed that treatment B was dominated by heterotrophs and treatments A and C remained heterotrophic, it would appear possible that heterotrophic capacity for resource use was not exceeded in any treatment and that the high nutrient treatments may have experienced trace nutrient limitation. Conversely, the B and C treatments both may have contained sufficient resources to support heterotrophic energy degradation and form autotrophic structures with remaining nutrients, and the C treatment eventually may have developed an autotrophic community, yielding positive values for GP that surpassed those of treatment B. More research is needed before any conclusive decisions can be reached regarding my unexpected results.

In both experiments, I did discover a positive relationship between initial DIN levels, measured as the sum of nitrate and ammonium, and PON, presumed to be an indicator of biomass formation in terms of nitrogen. Although there was a large standard deviation for the PON measurement for treatment C of the second experiment, total PON increased with increased initial values of DIN for both experiments, (Figs. 17, 18). This suggested a clear impact of available nutrients on the formation of biomass to catalyze energy degradation, and the correlation between PON and oxygen consumption, or respiration, revealed the ability of higher concentrations of biomass to further dissipate energy gradients. The amount of oxygen respired showed a strong positive relation to PON in the first experiment (Fig. 19). The second experiment likewise revealed a general increase in R with increased nitrogen biomass (Fig. 20). Whereas the values for R used to determine the relationship between R and PON in the first experiment were based on R and PON measured 12 d after nutrient addition, the values for PON in the second experiment reflect samples collected after 5 d, and R is averaged for 7-9 d after nutrient addition. However, the exact value of $-246 \mu\text{M O}_2/\text{d}$ calculated for R on the fifth day for treatment B does not alter the seemingly low PON concentration compared to the system's value for R, with measured PON less than that of treatment A. Yet, the general trend for both experiments revealed that greater respiratory activity occurred when more biomass was present for energy degradation.

In conclusion, my results demonstrated an overall dominance of heterotrophic metabolism in both microcosm experiments in accordance with my expectations based on MEP, particularly given the GP of $0 \mu\text{M O}_2/\text{d}$ and the minor contribution of autotrophic carbon to the total POC measured in all treatments except treatment B of the second experiment. Nutrient additions clearly impacted the metabolic activity of the systems, with increased respiration and DOC consumption at high nutrient levels. However, the ability of systems to allocate excess nutrients to autotrophic structures requires additional research due to the lack of autotrophy observed in the highest nutrient addition treatment of the second experiment, particularly given the observation of autotrophy in the intermediate nutrient treatment. For further analysis of the potential for autotrophic and heterotrophic development, data should be collected over time to determine whether or not the microcosms have fully stabilized and to monitor any changes in community dynamics over time. Also, research could be conducted in which nutrients are added in excess of glucose, but total glucose additions are low, thereby minimizing the potential for heterotrophic metabolism to cause trace nutrient limitation. Simultaneously, measurements of

iron, magnesium, and other trace nutrients could be conducted to assess the potential for autotrophic or heterotrophic limitation by these substances. In all, my results suggested the need for further experimentation and observation. However, the significant heterotrophic metabolism seen in this investigation, based on my analysis that heterotrophs are more efficient at maximizing energy degradation, supported my prediction based on MEP that heterotrophs will be selected for due to their greater ability to degrade energy. Ultimately, research may show that MEP can be used as a guiding principle for ecological studies, as envisioned by Schneider and Kay (1994). As seen in its utility for predicting the dominant metabolic pathways and types of structure formed in microcosms, the MEP hypothesis holds great promise for increasing our ability to understand and predict community structure and function.

ACKNOWLEDGMENTS

I would like to thank Dr. Joe Vallino for his extensive assistance and advice throughout this investigation. I also would like to acknowledge Clara Funk, Allison Burce, Laura Wittman, and Richard McHorney for their assistance. This research has been funded by the Semester in Environmental Science of the Marine Biological Laboratory, and I would like to acknowledge the Marine Biological Laboratory for use of all equipment and laboratory space.

LITERATURE CITED

- Fath, B. D., B. C. Patten, and J. S. Choi. 2001. Complementarity of ecological goal functions. *Journal of Theoretical Biology* **208**: 493-506.
- Gilpin, L. C., K. Davidson, and E. Roberts. 2004. The influence of changes in nitrogen: silicon ratios on diatom growth dynamics. *Journal of Sea Research* **51**:21-35.
- Hashsham, S. A., A. S. Fernandex, S. L. Dollhopf, F. B. Dazzo, R. F. Hickey, J. M. Tiedge, and C. S. Criddle. 2000. Parallel processing of substrate correlates with greater functional stability in methanogenic bioreactor communities perturbed by glucose. *Applied and Environmental Microbiology* **66(9)**:4050-4057.
- Lorenzen, C. J. 1967. Determination of chlorophyll and pheo-pigments: spectrophotometric equations. *Limnology and Oceanography* **12(2)**:343-346.
- Madigan, M. T., J. M. Martinko, and J. Parker. 2000. *Brock Biology of Microorganisms*, 9th ed. Prentice Hall, Upper Saddle River, NJ, 991 pp.
- Peltzer, E. T., and P. G. Brewer. 1993. Some practical aspects of measuring DOC – sampling artifacts and analytical problems with marine samples. *Marine Chemistry* **41**:243-252.
- Salthe, S. N. 2003. Infodynamics, a developmental framework for ecology/economics. *Conservation Ecology* **7(3)**:3. <<http://www.consecol.org/vol7/iss3/art3/>>.
- Schlesinger, W. H. 1997. *Biogeochemistry: An Analysis of Global Change*, 2nd ed. Academic Press, San Diego, CA, 588 pp.
- Schneider, E. D., and J. J. Kay. 1994. Complexity and thermodynamics: towards a new ecology. *Futures* **24(6)**:626-647.
- Schrödinger, E. 1945. *What is life? The physical aspect of the living cell*. The Macmillan Company, NY, NY, 91 pp.
- Solórzano, L. 1969. Determination of ammonia in natural waters by the phenolhypochlorite method. *Limnology and Oceanography* **14(5)**:799-801.
- Shapiro, J. A. 1998. Thinking about bacterial populations as multicellular organisms. *Annual Review of Microbiology* **52**:81-104.
- Talaro, K. P. 2005. *Foundations in microbiology*, 5th ed. McGraw-Hill, NY, NY, 831 pp.

- Valiela, I. 1995. *Marine Ecological Processes*, 2nd ed. Springer, NY, NY, 686 pp.
- Vallino, J. J. 2003. Modeling microbial consortiums as distributed metabolic networks. *Biological Bulletin* **204**: 174-179.
- Whitman, W. B., D. C. Coleman, and W. J. Wiebe. 1998. Prokaryotes: The unseen majority. *Proceedings of the National Academy of Sciences* **95**: 6578-6583.

APPENDIX

Treatment	KNO ₃		Na ₂ SiO ₃ · 9H ₂ O		KH ₂ PO ₄	
	Concentration (μM)	Mass (g)	Concentration (μM)	Mass (g)	Concentration (μM)	Mass (g)
A	0.00	0.0000	0.00	0.0000	0.00	0.0000
B	10.00	0.0183	15.00	0.0774	0.63	0.0015
C	50.00	0.0917	75.00	0.3868	3.13	0.0077
D	100.00	0.1834	150.00	0.7736	6.25	0.0154

Table 1. Mass values and concentrations used for the single nutrient addition made to microcosms in the first experiment. Values refer to the initial concentrations before water was removed for samples. One replicate was made for each treatment, but results do not include the values for the second microcosm in the C and D treatments.

Treatment	KNO ₃		Na ₂ SiO ₃ · 9H ₂ O		KH ₂ PO ₄	
	Concentration (μM)	Mass (g)	Concentration (μM)	Mass (g)	Concentration (μM)	Mass (g)
A	10.00	0.0183	15.00	0.0774	0.63	0.0015
B	100.00	0.1834	150.00	0.7736	6.25	0.0154
C	1000.00	1.8341	1500.00	7.7361	62.50	0.1544

Table 2. Mass values and concentrations used for the single nutrient addition made to the second set of microcosms for experiment two. One replicate was made of each treatment. Values refer to the initial concentrations before water was removed for samples.

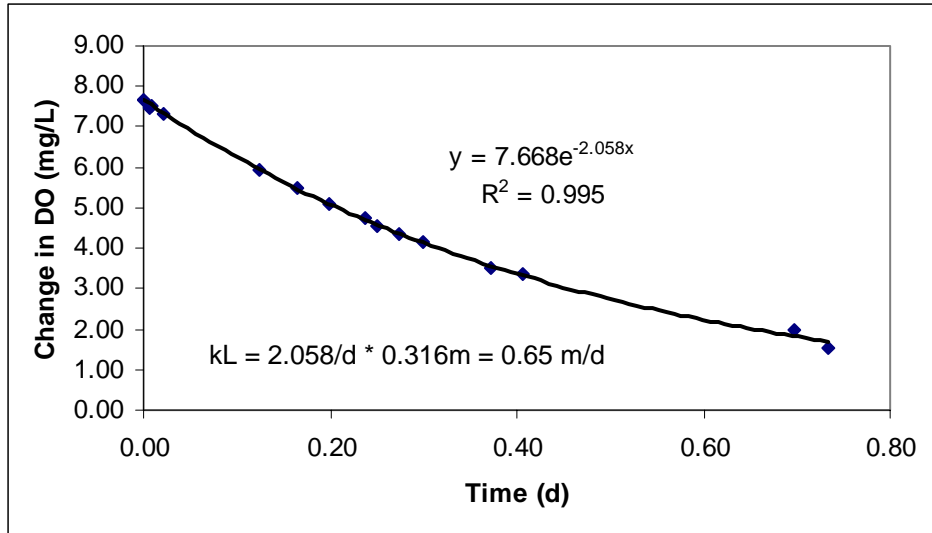


Figure 1. Calculation of piston velocity in seawater from Eel Pond.

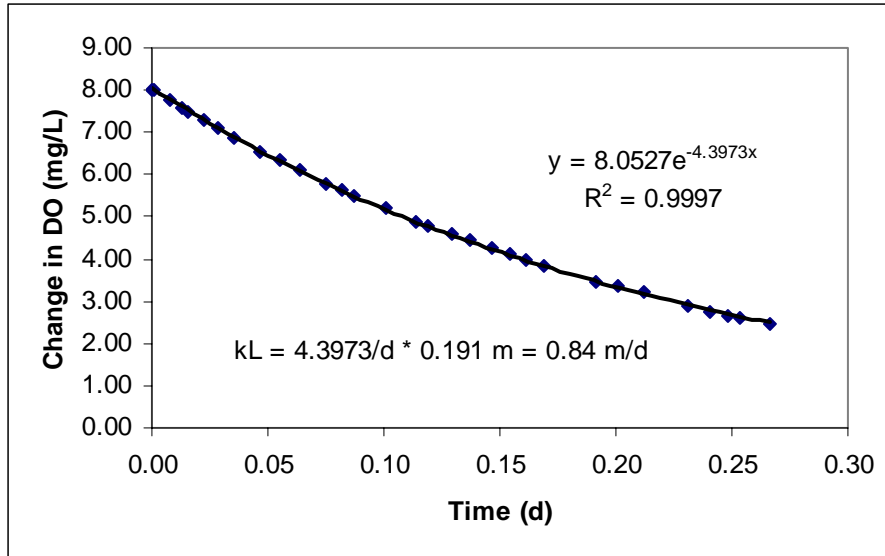


Figure 2. Calculation of piston velocity in a bucket of artificial seawater.

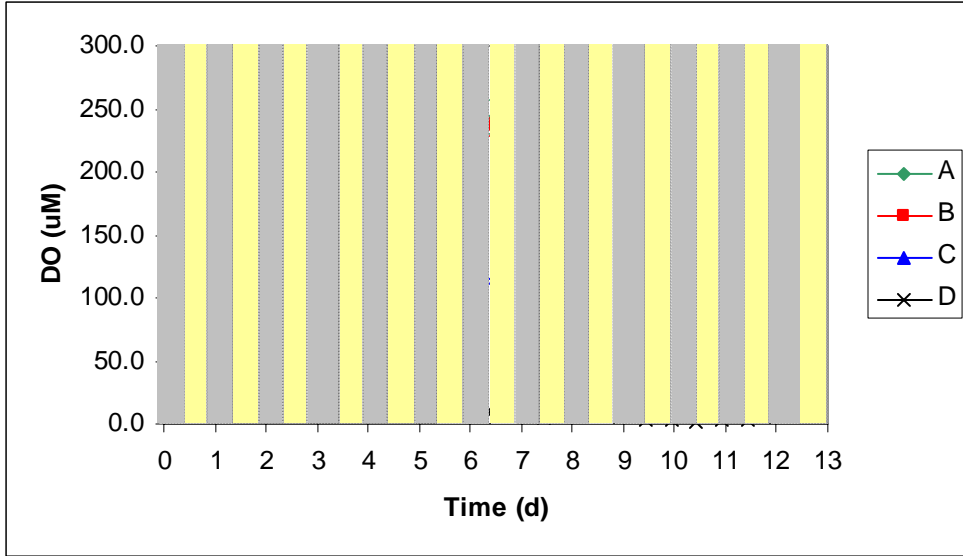


Figure 3. Concentrations of DO throughout the first experiment. Yellow columns represent the 12 h during which the lights were on each day, and gray columns represent the subsequent 12 h of darkness. Values for treatments A and B are based on the average for the two replicate microcosms, and bars depict the standard deviation for these treatments.

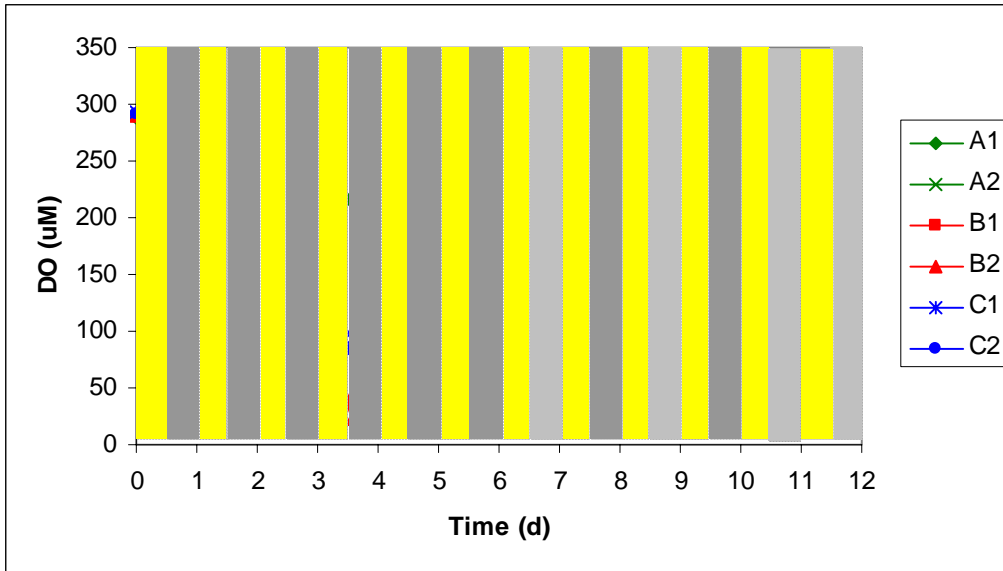


Figure 4. Concentrations of DO throughout the second experiment. Yellow columns represent the 12 h during which the lights were on each day, and gray columns represent the subsequent 12 h of darkness. After 7 d, the second replicate of microcosms (A2, B2, and C2) were excluded from light for the remainder of the experiment.

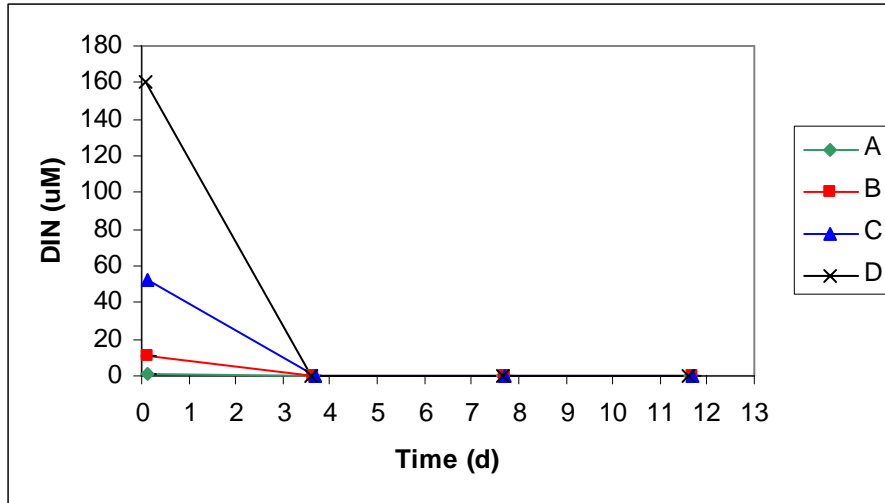


Figure 5. Decline in DIN, approximated as the sum of nitrate and ammonium, for the four treatments of the first experiment. Values for A and B represent the average of two microcosms. Standard deviations were plotted as error bars but the values were minimal, with a maximum of 0.04 for the A treatment at any point in time, and a maximum of 0.22 in the B treatment at any point in time.

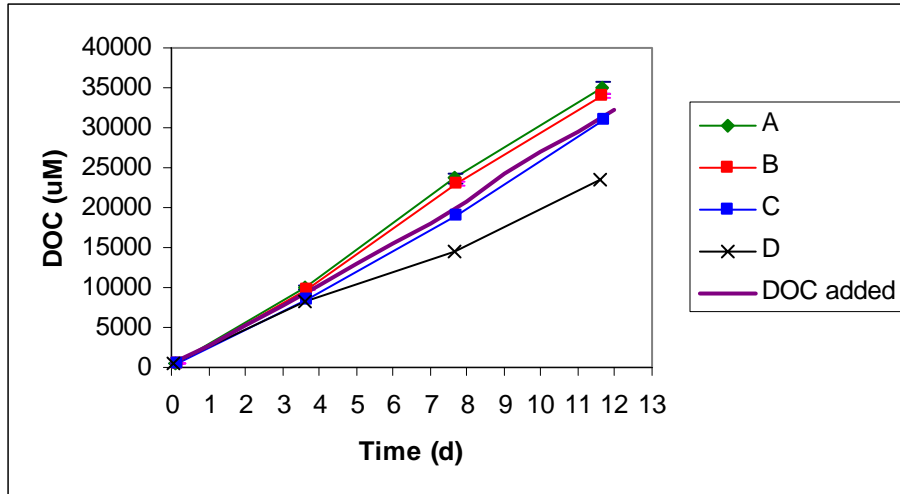


Figure 6. Concentrations of DOC over time in each treatment. Total DOC added is shown, with concentrations determined for the amount of water remaining in the microcosms after sampling. Values for treatments A and B represent the average for two replicate microcosms. Standard deviation bars are depicted for treatments A and B, with a maximum standard deviation of 779 for treatment A and 291 for treatment B. Approximately 121 μM DOC was measured in a sample of seawater to which no glucose additions were made.

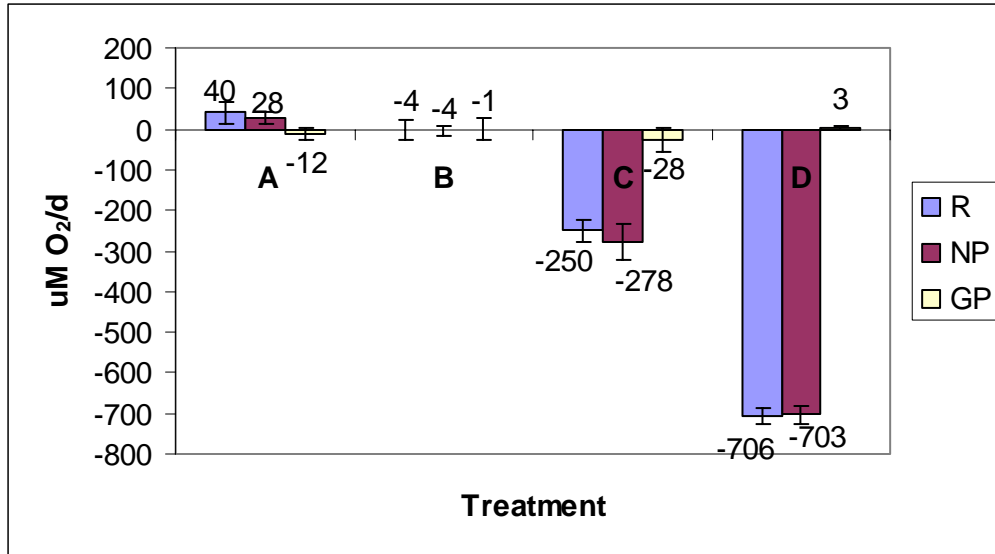


Figure 7. Average R, NP, and GP for 7-9 d after initial nutrient additions in the second experiment. Values for treatments A and B represent the average found for the two microcosms of each treatment. Bars represent the standard deviation for all treatments over this time.

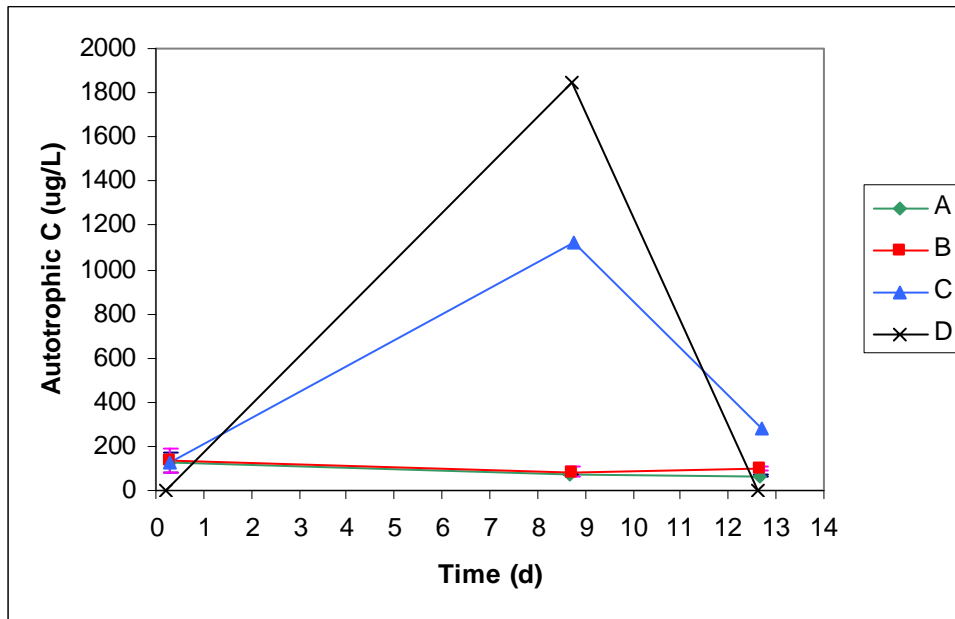


Figure 8. Autotrophic carbon over time for the four treatments of experiment 1, as estimated from measurements of chl *a* and an assumed ratio of 50 $\mu\text{g C}$:1 $\mu\text{g chl } a$. Values for treatments A and B represent the average for two replicate microcosms. Bars depict the standard deviation for treatments A and B, with all values for standard deviation less than 60 $\mu\text{g C/L}$.

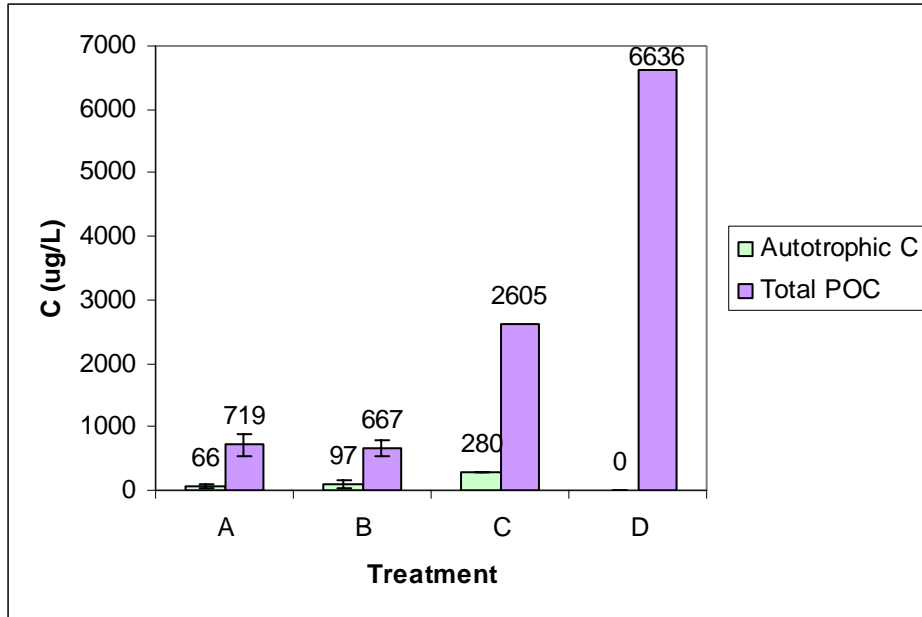


Figure 9. Comparison of estimated autotrophic carbon and measured POC in the four treatments of the first experiment approximately 12.5 d after nutrient additions. Values for treatments A and B represent the average found for the two microcosms of each treatment, and the bars shown represent the standard deviation for these two treatments.

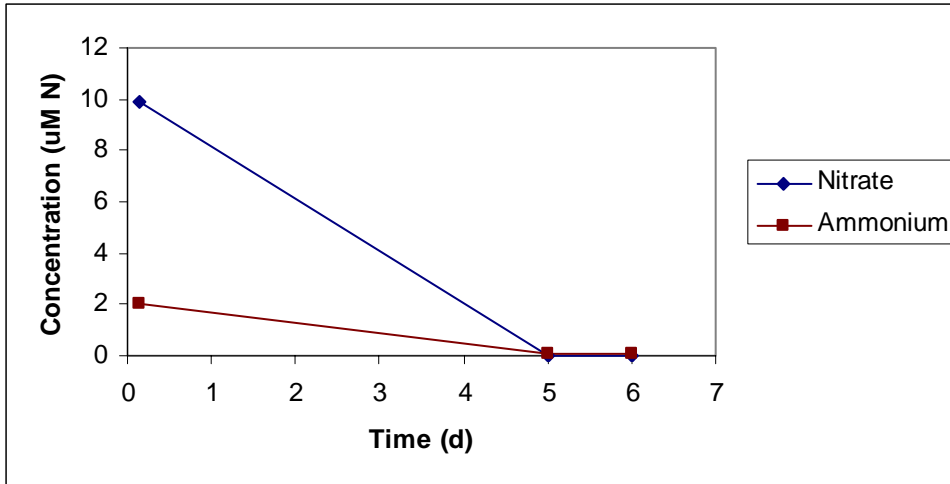


Figure 10. Concentrations of nitrate and ammonium for treatment A of the second experiment. Values represent the average of the two A microcosms. Standard deviation was plotted as error bars, but the values were minimal, with a maximum standard deviation of 0.005 for nitrate and for ammonium.

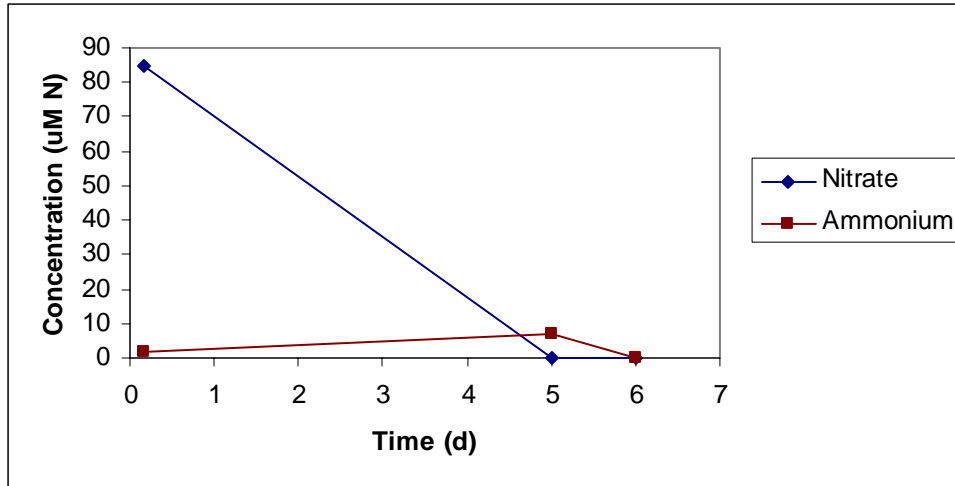


Figure 11. Concentrations of nitrate and ammonium for treatment B of the second experiment. Values represent the average of the two B microcosms. Standard deviation was plotted as error bars, but the values were minimal, with a maximum standard deviation of 0.004 for nitrate and ammonium.

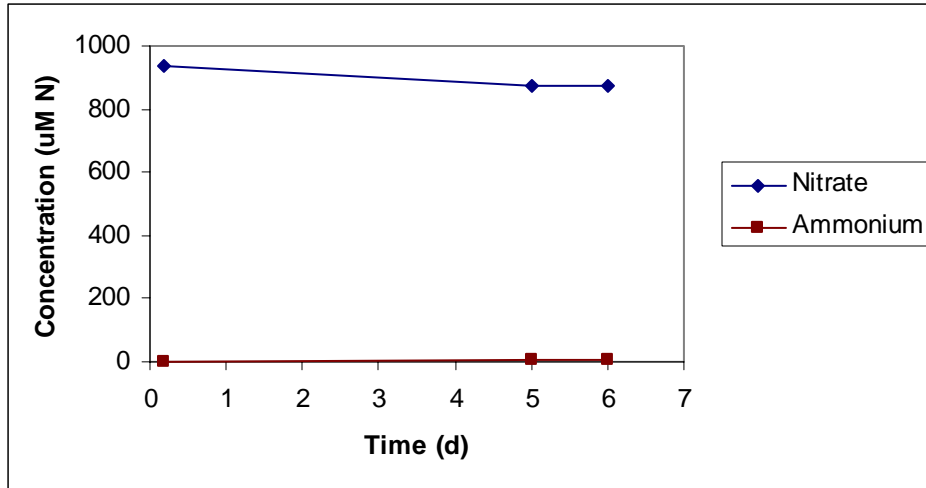


Figure 12. Concentrations of nitrate and ammonium for treatment C of the second experiment. Values represent the average for the two C treatments. Standard deviation was plotted as error bars, but the values were minimal, with a maximum standard deviation of 0.23 for nitrate and 0.12 for ammonium.

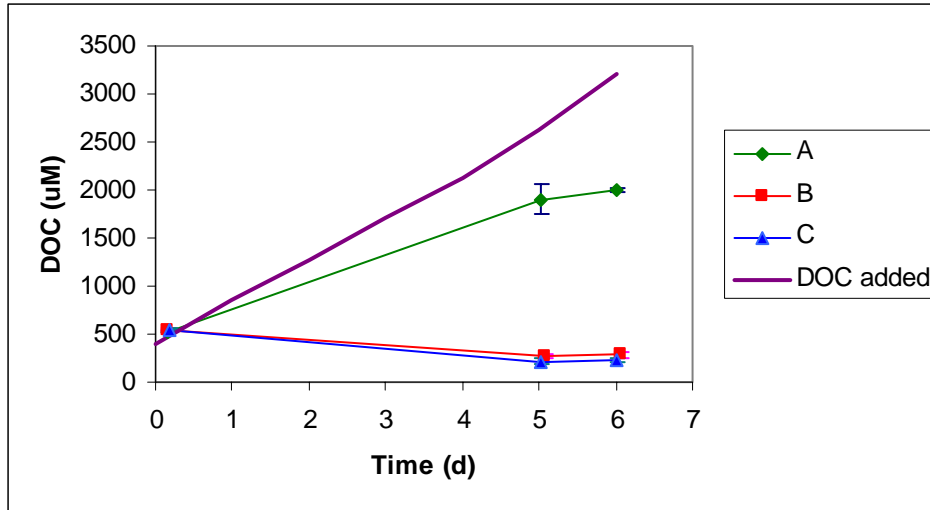


Figure 13. Concentration of DOC over time and total DOC added for the second experiment, with average values for the two microcosms in each treatment and standard deviations shown by the error bars. Approximately 141 μM DOC was measured in a sample of seawater to which no glucose additions were made.

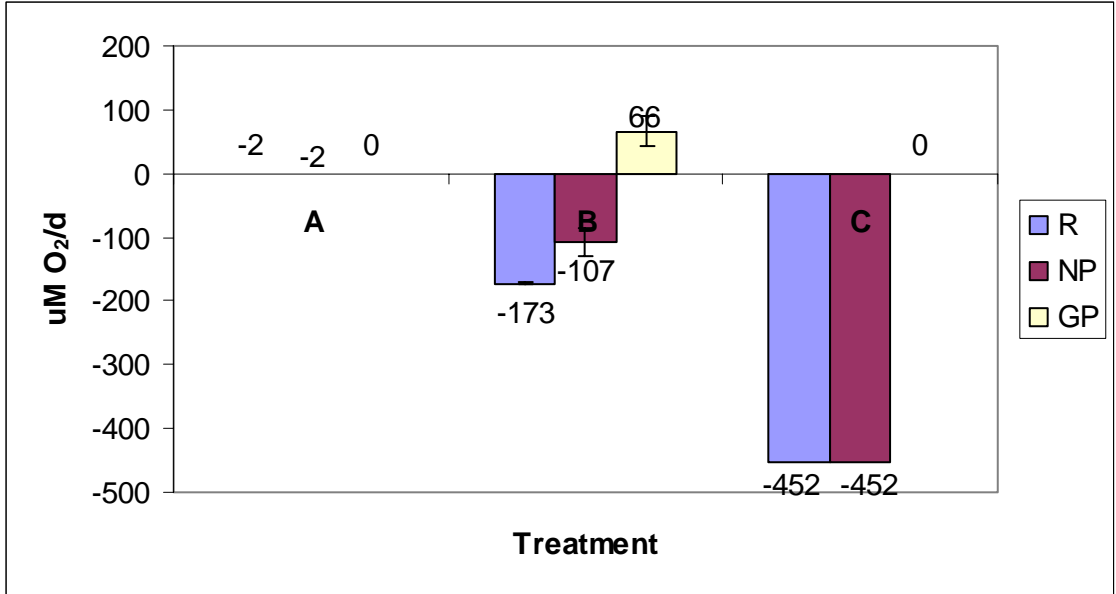


Figure 14. Values for R, NP, and GP for the microcosms kept in the light in the second experiment. Values represent the average over days 7-9. Standard deviation values are shown for treatment B. Rates of R, NP, and GP for treatments A and C were determined based on a visual estimate from the graphs of DO of the value of $O_2(avg)$, and the standard deviation was not calculated for these treatments.

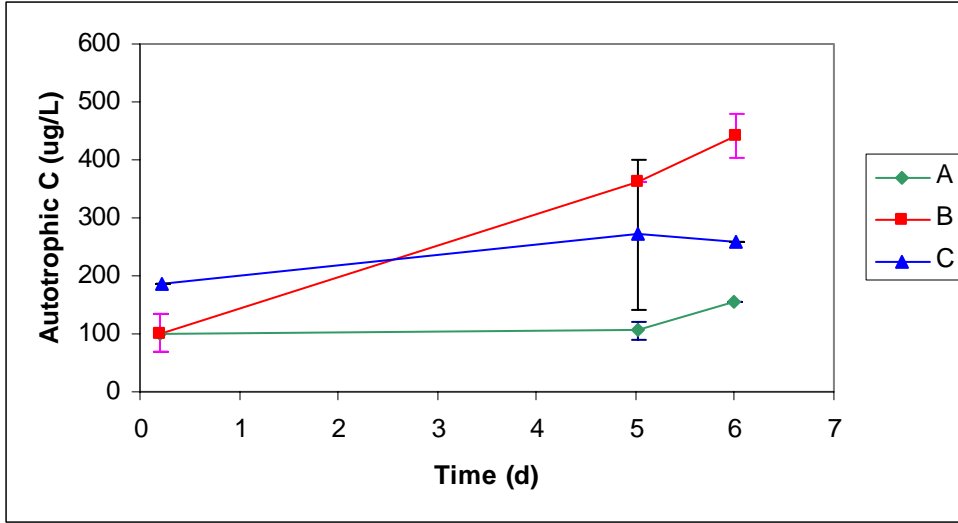


Figure 15. Autotrophic carbon over time for the three treatments of the second experiment, as estimated from measurements of chl *a* and an assumed ratio of 50 $\mu\text{g C}$:1 $\mu\text{g chl } a$. Values are the average found for the two microcosms in each treatment, with standard deviations shown by the error bars.

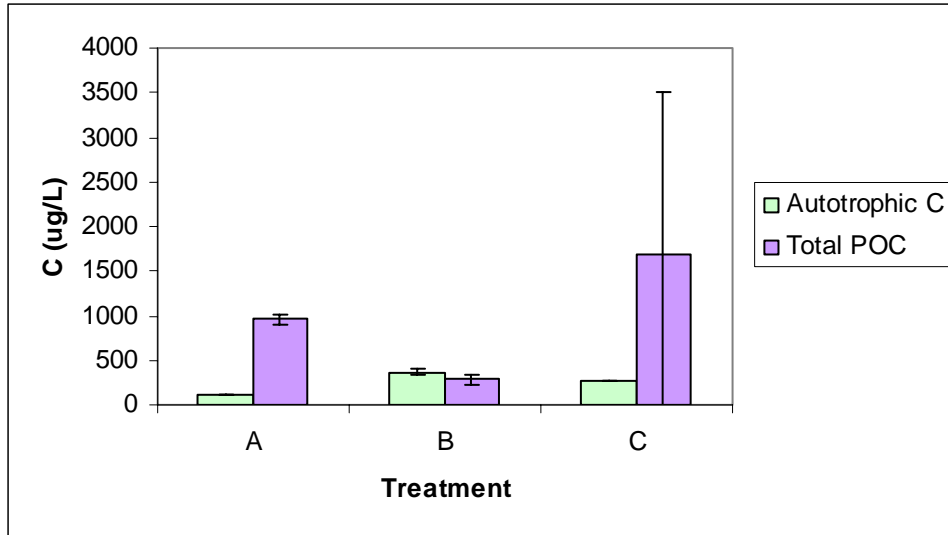


Figure 16. Comparison of estimated autotrophic carbon and measured POC in the second experiment approximately 5 d after nutrient additions. Values are the average found for the two microcosms in each treatment, with standard deviations shown by the error bars.

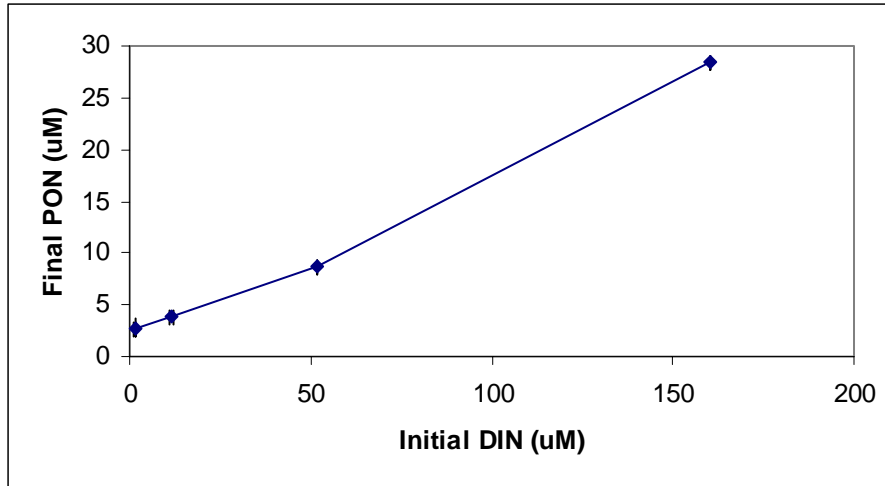


Figure 17. Total PON for the final measurement conducted after 12 d, shown as a function of the original measurement of DIN (approximated as the sum of nitrate and ammonium) for the first experiment. Values for treatments A and B (with initial DIN of approximately 0 and 10 μM DIN, respectively) represent the average for the two microcosms with these treatments. Standard deviations were graphed as error bars for treatments A and B, but values were less than 1.

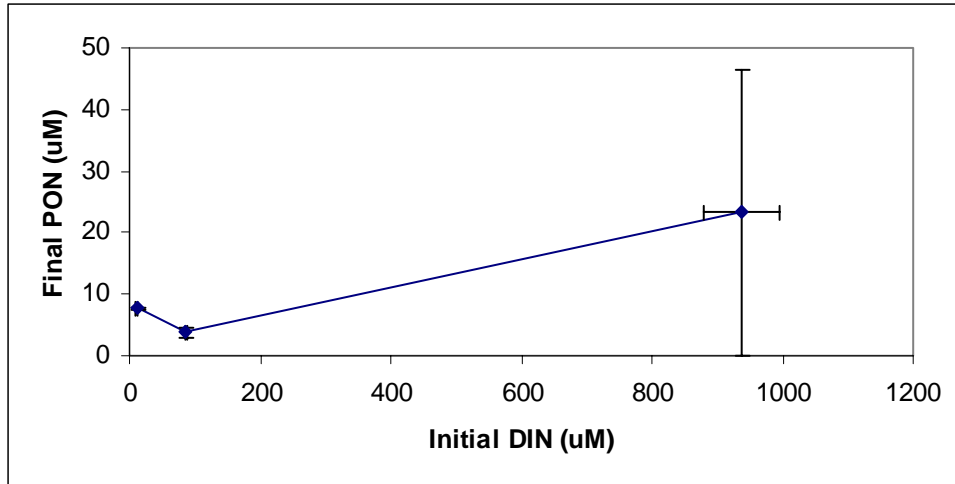


Figure 18. Total PON for the last measurement conducted after 5 d, shown as a function of the original measurement of DIN (approximated as the sum of nitrate and ammonium) for the second experiment. Values for all treatments represent the average of two microcosms, with standard deviations depicted by the error bars.

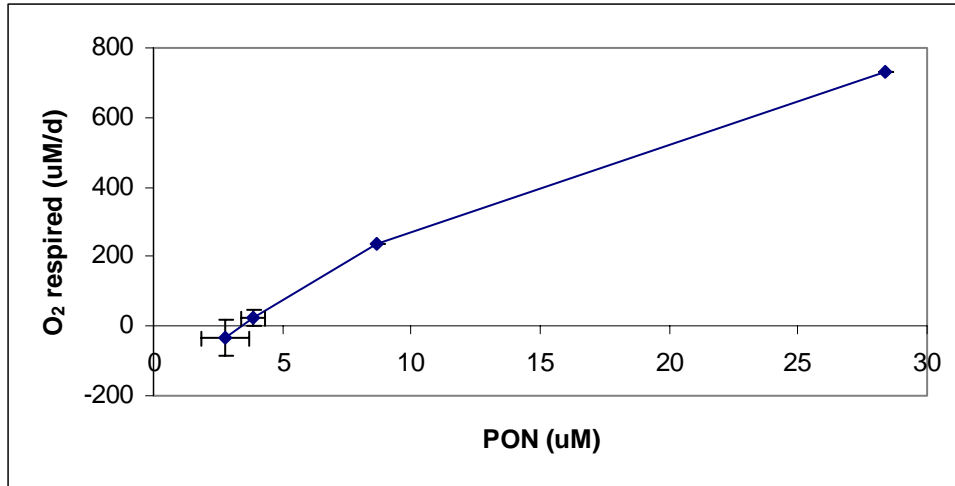


Figure 19. Oxygen respired as a function of PON for all four treatments after 12 d in the first experiment. Oxygen respired is plotted as the opposite of calculated R (typically negative) to show the positive relationship between the amount of oxygen consumed and total PON. Results for treatments A and B (with PON concentrations of approximately 3 and 4 μM , respectively) represent the average for two replicate microcosms, with standard deviations shown by the error bars.

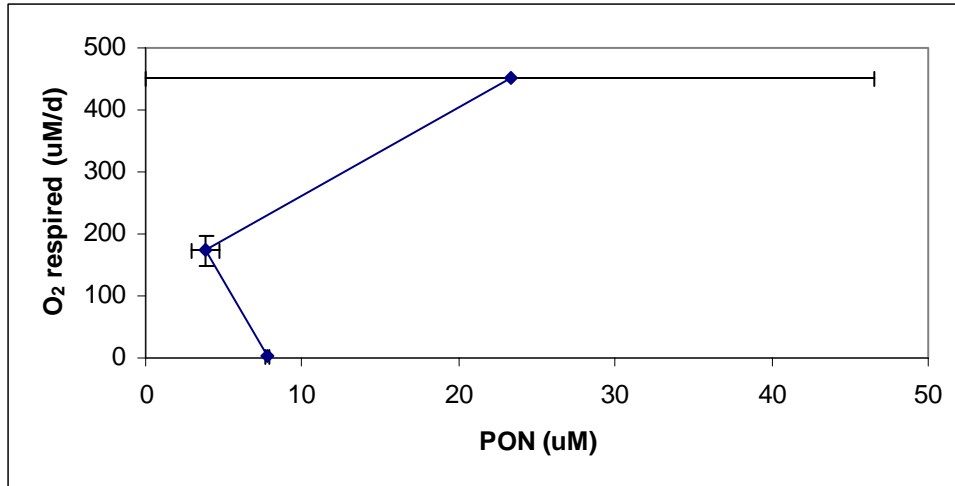


Figure 20. Oxygen respired as a function of PON for all four treatments after 5 d of the second experiment. Oxygen respired is plotted as the opposite of calculated R (a negative value) to show the positive relationship between the amount of oxygen consumed and total PON. Concentrations of PON represent the average for two replicate microcosms, with standard deviations shown for PON concentration in all microcosms. Values for respiration represent the average calculated for the microcosms kept in the light over days 7-9, with the standard deviation shown for treatment B.